

161. Photoactive Cryptands

Crystal Structure of the Sodium Cryptate of the Tris(phenanthroline) Macrobicyclic Ligand

by Aimery Caron¹⁾, Jean Guilhelm, Claude Riche, and Claudine Pascard

Institut de Chimie des Substances Naturelles, C.N.R.S., F-91190 Gif-sur-Yvette

and Béatrice Alpha, Jean-Marie Lehn^{*}, and Juan-Carlos Rodriguez-Ubis²⁾

Institut Le Bel, Université Louis Pasteur, 4, rue Blaise Pascal, F-67000 Strasbourg

Dedicated to the memory of Professor *Jerry Donohue*

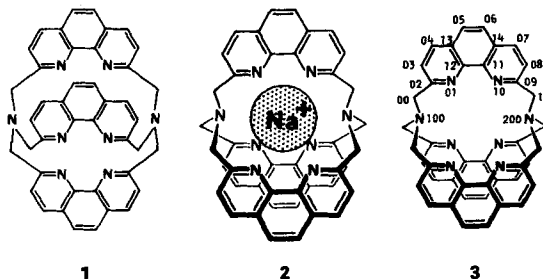
(19.VI.85)

The crystal structure of the complex $[\text{phen} \cdot \text{phen} \cdot \text{phen}] \cdot \text{NaBr} \cdot 2 \text{CHCl}_3$ of the macrobicyclic ligand **1** has been determined. The complex is of cryptate type, the Na^+ cation being contained in the molecular cavity of **1** and coordinated to all eight N-atoms. The ligand has a propeller shape and interconverts in solution between the two enantiomeric helical forms.

The synthesis of the NaBr complexes of macrobicyclic ligands incorporating 2,2'-bipyridine and 1,10-phenanthroline groups has been reported recently [1]. On the basis of the results obtained and by analogy with the earlier work on cation cryptates [2–4], they were considered to be sodium cryptates, formed by inclusion of the Na^+ cation in the molecular cavity of the ligand. Such complexes combine the inclusion nature of cryptates with the photoactivity of the bipyridine and phenanthroline groups.

We now describe the crystal structure of the sodium complex of the macrobicyclic ligand $[\text{phen} \cdot \text{phen} \cdot \text{phen}]$ (**1**).

Structure of the Complex $1 \cdot \text{NaBr} \cdot 2 \text{CHCl}_3$. – The crystal structure shows that the sodium complex of **1** is of cryptate type, $[\text{Na}^+ \subset \mathbf{1}]$, i.e. **2**, with the Na^+ cation contained



¹⁾ Permanent address: College of the Virgin Islands, St. Thomas, Virgin Islands 00801, USA.

²⁾ Permanent address: Universidad Autonoma de Madrid, Facultad de Ciencias, 28049-Madrid, Spain.

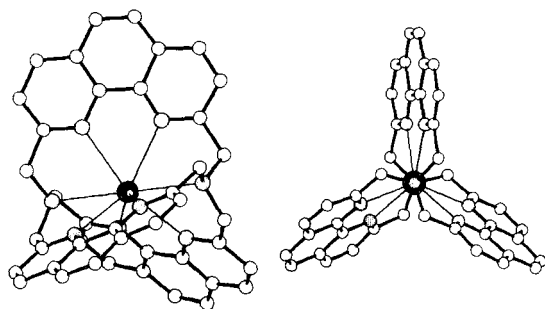


Fig. 1. Two views of the crystal structure of the sodium cryptate [$\text{Na}^+ \subset 1$], i.e. **2**. (a) Left: view into the cavity, showing the coordination of the Na^+ ion to the eight N-sites; (b) right: projection upon a plane perpendicular to the $\text{N}(100) \cdots \text{Na}^+ \cdots \text{N}(200)$ axis, showing the propeller-shaped conformation.

Table 1. Na^+ Bond Lengths [\AA] in the Cryptate **2** $\text{Br} \cdot 2\text{CHCl}_3^a$

$\text{Na}^+ - \text{N}(100)$	2.774 (10)	$\text{Na}^+ - \text{N}(01)$	2.695 (11)	$\text{Na}^+ - \text{N}'(10)$	2.677 (8)
$\text{Na}^+ - \text{N}(200)$	2.805 (10)	$\text{Na}^+ - \text{N}(10)$	2.731 (10)	$\text{Na}^+ - \text{N}''(01)$	2.722 (10)
		$\text{Na}^+ - \text{N}'(01)$	2.696 (9)	$\text{Na}^+ - \text{N}''(10)$	2.702 (11)

^{a)} For numbering, see 3.

in the molecular cavity of **1** and well separated from the Br^- counteranion. The complex cation is a racemic mixture of propeller-shaped complexes of approximate symmetry 3 where the linear bonds $\text{N}(100) \cdots \text{Na}^+ \cdots \text{N}(200)$ represent the shaft and each planar phenanthroline group a blade of the propeller (Fig. 1). The complex lacks a mirror plane of symmetry as the phenanthroline planes are inclined by $16.3(4)^\circ$ from the shaft axis. The enclosed Na^+ cation is bounded by the six N-atoms of the phenanthroline groups at $2.70(1) \text{ \AA}$ and the two bridge N-atoms at $2.79(1) \text{ \AA}$ (Table 1). These $\text{Na}^+ - \text{N}$ bond lengths are longer than those found in an open bis-phenanthroline complex [5] of a hexacoordinated Na^+ ion with four $\text{Na}^+ \cdots \text{N}$ distances of $2.50(4) \text{ \AA}$; presumably, the longer distances are due to the rigidity of the cryptand **1** and the higher coordination of the Na^+ ion.

Table 2. Na^+ Bond Angles [$^\circ$] in the Cryptate **2** $\text{Br} \cdot 2\text{CHCl}_3^a$

$\text{N}(100) - \text{Na}^+ - \text{N}(01)$	62.2 (3)	$\text{N}(01) - \text{Na}^+ - \text{N}'(10)$	114.6 (3)
$\text{N}(100) - \text{Na}^+ - \text{N}'(01)$	61.2 (3)	$\text{N}'(01) - \text{Na}^+ - \text{N}''(10)$	109.9 (3)
$\text{N}(100) - \text{Na}^+ - \text{N}'(10)$	119.5 (3)	$\text{N}''(01) - \text{Na}^+ - \text{N}(10)$	113.4 (3)
$\text{N}(100) - \text{Na}^+ - \text{N}''(01)$	60.7 (3)		
$\text{N}(200) - \text{Na}^+ - \text{N}(10)$	60.5 (3)	$\text{N}(100) - \text{Na}^+ - \text{N}(10)$	119.6 (3)
$\text{N}(200) - \text{Na}^+ - \text{N}'(10)$	60.7 (3)	$\text{N}(100) - \text{Na}^+ - \text{N}''(10)$	118.5 (3)
$\text{N}(200) - \text{Na}^+ - \text{N}''(10)$	61.1 (3)	$\text{N}(200) - \text{Na}^+ - \text{N}(01)$	118.1 (3)
$\text{N}(01) - \text{Na}^+ - \text{N}(10)$	60.1 (3)	$\text{N}(200) - \text{Na}^+ - \text{N}'(01)$	118.9 (3)
$\text{N}'(01) - \text{Na}^+ - \text{N}'(10)$	61.0 (3)	$\text{N}(200) - \text{Na}^+ - \text{N}''(01)$	119.0 (3)
$\text{N}''(01) - \text{Na}^+ - \text{N}''(10)$	60.5 (3)		
$\text{N}(01) - \text{Na}^+ - \text{N}'(01)$	101.4 (3)	$\text{N}(01) - \text{Na}^+ - \text{N}''(10)$	143.8 (3)
$\text{N}(10) - \text{Na}^+ - \text{N}'(10)$	99.4 (3)	$\text{N}'(01) - \text{Na}^+ - \text{N}(10)$	146.5 (3)
$\text{N}'(01) - \text{Na}^+ - \text{N}''(01)$	96.2 (3)	$\text{N}''(01) - \text{Na}^+ - \text{N}'(10)$	141.6 (3)
$\text{N}'(10) - \text{Na}^+ - \text{N}''(10)$	96.6 (3)		
$\text{N}''(01) - \text{Na}^+ - \text{N}(01)$	99.2 (3)		
$\text{N}''(10) - \text{Na}^+ - \text{N}(10)$	98.5 (3)	$\text{N}(100) - \text{Na}^+ - \text{N}(200)$	179.6 (2)

^{a)} For numbering, see 3.

Table 3. Angles [°] between the Bonds to the N(100)–Na⁺–N(200) Axis of the Cryptate 2 Br · 2CHCl₃ upon the Perpendicular Plane, all ± 0.5°^{a)}

C(00)–(N(100)–Na ⁺ –N(200))–C'(15)	31.8°	C(00)–(N(100)–Na ⁺ –N(200))–N(01)	– 36.0
C'(00)–(N(100)–Na ⁺ –N(200))–C''(15)	35.6	C(15)–(N(100)–Na ⁺ –N(200))–N(10)	33.8
C''(00)–(N(100)–Na ⁺ –N(200))–C(15)	32.1	C'(00)–(N(100)–Na ⁺ –N(200))–N'(01)	– 30.4
N(01)–(N(100)–Na ⁺ –N(200))–N(10)	– 18.5	C'(15)–(N(100)–Na ⁺ –N(200))–N'(10)	36.4
N'(01)–(N(100)–Na ⁺ –N(200))–N'(10)	– 18.9	C''(00)–(N(100)–Na ⁺ –N(200))–N''(01)	– 35.9
N''(01)–(N(100)–Na ⁺ –N(200))–N''(10)	– 18.4	C''(15)–(N(100)–Na ⁺ –N(200))–N''(10)	32.3

^{a)} For numbering, see 3.

The Na⁺ bond angles (Table 2) can be grouped into six average values: nine at 60.9 (5)°, six at 98.6 (1.8)°, three at 112.6 (2.0)°, six at 118.9 (3)°, three at 144.0 (2.0)°, and one at 179.6 (2)° for the N(100)···Na⁺···N(200) angle. A projection of the cryptate upon a plane perpendicular to the N(100)···Na⁺···N(200) axis (Fig. 1b) reveals that all six NaN-bonds and six CN-bonds are well distributed around 360° and avoid eclipsing one another. The CN-bonds have projection angles clustering around 32(2)°, those of the NaN-bonds 18.6(2)°, while those angles between the NaN- and CN-bonds average 34(2)° (Table 3).

Within experimental error, all three phenanthroline groups have the same bond lengths and angles (Tables 4 and 5) which agree well with the published values for *o*-phenanthroline [6]. The least-square planes for the three phenanthroline groups are defined in Table 6. The average atomic deviation from these planes is 0.013 Å and the largest deviation is 0.084 Å for C'(07).

Table 4. Bond Distances [Å] with *e.s.d.*'s for 2 Br · 2CHCl₃

N(100)–C(00)	1.48 (2)	C'(00)–C'(02)	1.52 (2)	C''(00)–C''(02)	1.51 (2)
N(100)–C'(00)	1.46 (1)	N'(01)–C'(02)	1.31 (1)	N''(01)–C''(02)	1.35 (1)
N(100)–C''(00)	1.46 (2)	N'(01)–C'(12)	1.38 (1)	N''(01)–C''(12)	1.33 (1)
N(200)–C(15)	1.46 (1)	C'(02)–C'(03)	1.41 (2)	C''(02)–C''(03)	1.39 (2)
N(200)–C'(15)	1.45 (1)	C'(03)–C'(04)	1.34 (2)	C''(03)–C''(04)	1.35 (2)
N(200)–C''(15)	1.48 (1)	C'(04)–C'(13)	1.38 (2)	C''(04)–C''(13)	1.41 (2)
		C'(05)–C'(06)	1.33 (2)	C''(05)–C''(06)	1.37 (2)
C(00)–C(02)	1.52 (2)	C'(05)–C'(13)	1.44 (2)	C''(05)–C''(13)	1.43 (2)
N(01)–C(02)	1.31 (2)	C'(06)–C'(14)	1.44 (2)	C''(06)–C''(14)	1.41 (2)
N(01)–C(12)	1.32 (2)	C'(07)–C'(08)	1.32 (2)	C''(07)–C''(08)	1.34 (2)
C(02)–C(03)	1.45 (2)	C'(07)–C'(14)	1.38 (2)	C''(07)–C''(14)	1.42 (2)
C(03)–C(04)	1.33 (2)	C'(08)–C'(09)	1.41 (2)	C''(08)–C''(09)	1.40 (2)
C(04)–C(13)	1.40 (2)	C'(09)–N'(10)	1.33 (1)	C''(09)–N''(10)	1.33 (1)
C(05)–C(06)	1.34 (2)	C'(09)–C'(15)	1.50 (2)	C''(09)–C''(15)	1.51 (2)
C(05)–C(13)	1.37 (2)	N'(10)–C'(11)	1.37 (1)	N''(10)–C''(11)	1.34 (1)
C(06)–C(14)	1.43 (2)	C'(11)–C'(12)	1.43 (2)	C''(11)–C''(12)	1.48 (1)
C(07)–C(08)	1.40 (2)	C'(11)–C'(14)	1.41 (2)	C''(11)–C''(14)	1.41 (2)
C(07)–C(14)	1.39 (2)	C'(12)–C'(13)	1.42 (2)	C''(12)–C''(13)	1.39 (2)
C(08)–C(09)	1.39 (2)				
C(09)–N(10)	1.34 (1)			C(20)–Cl(21)	1.75 (1)
C(09)–C(15)	1.52 (2)			C(20)–Cl(22)	1.74 (1)
N(10)–C(11)	1.39 (1)			C(20)–Cl(23)	1.76 (1)
C(11)–C(12)	1.42 (2)			C(30)–Cl(31)	1.67 (3)
C(11)–C(14)	1.40 (2)			C(30)–Cl(32)	1.66 (2)
C(12)–C(13)	1.49 (2)			C(30)–Cl(33)	1.71 (2)

Table 5. Bond Angles [°] with *e.s.d.*'s for **2 Br · 2CHCl₃**

C(00)–N(100)–C'(00)	108(1)	C'(02)–N'(01)–C'(12)	117(1)	N(100)–C''(00)–C''(02)	111(1)
C(00)–N(100)–C''(00)	111(1)	C'(00)–C'(02)–N'(01)	118(1)	C''(02)–N''(01)–C''(12)	118(1)
C'(00)–N(100)–C''(00)	111(1)	C'(00)–C'(02)–C'(03)	118(1)	C''(00)–C''(02)–N''(01)	117(1)
C(15)–N(200)–C'(15)	111(1)	N'(01)–C'(02)–C'(03)	125(1)	C''(00)–C''(02)–C''(03)	122(1)
C(15)–N(200)–C''(15)	109(1)	C'(02)–C'(03)–C'(04)	116(1)	N''(01)–C''(02)–C''(03)	122(1)
C'(15)–N(200)–C''(15)	111(1)	C'(03)–C'(04)–C'(13)	123(1)	C''(02)–C''(03)–C''(04)	120(1)
N(100)–C(00)–C(02)	110(1)	C'(06)–C'(05)–C'(13)	119(1)	C''(03)–C''(04)–C''(13)	120(1)
C(02)–N(01)–C(12)	120(1)	C'(05)–C'(06)–C'(14)	123(1)	C''(06)–C''(05)–C''(13)	117(1)
C(00)–C(02)–N(01)	120(1)	C'(08)–C'(07)–C'(14)	122(1)	C'(05)–C''(06)–C''(14)	123(1)
C(00)–C(02)–C(03)	119(1)	C'(07)–C'(08)–C'(09)	120(1)	C''(08)–C''(07)–C''(14)	118(1)
N(01)–C(02)–C(03)	122(1)	C'(08)–C'(09)–N'(10)	122(1)	C''(07)–C''(08)–C''(09)	121(1)
C(02)–C(03)–C(04)	119(1)	C'(08)–C'(09)–C'(15)	121(1)	C''(08)–C''(09)–N''(10)	123(1)
C(03)–C(04)–C(13)	123(1)	N'(10)–C'(09)–C'(15)	118(1)	C''(08)–C''(09)–C''(15)	119(1)
C(06)–C(05)–C(13)	123(1)	C'(09)–N'(10)–C'(11)	118(1)	N''(10)–C''(09)–C''(15)	118(1)
C(05)–C(05)–C(14)	120(1)	N'(10)–C'(11)–C'(12)	118(1)	C''(09)–N''(10)–C''(11)	117(1)
C(08)–C(07)–C(14)	119(1)	N'(10)–C'(11)–C'(14)	123(1)	N''(10)–C''(11)–C''(12)	118(1)
C(07)–C(08)–C(09)	118(1)	C'(12)–C'(11)–C'(14)	119(1)	N''(10)–C''(11)–C''(14)	124(1)
C(08)–C(09)–N(10)	124(1)	N'(01)–C'(12)–C'(11)	119(1)	C''(12)–C''(11)–C''(14)	117(1)
C(08)–C(09)–C(15)	121(1)	N'(01)–C'(12)–C'(13)	121(1)	N''(01)–C''(12)–C''(11)	117(1)
N(10)–C(09)–C(15)	115(1)	C'(11)–C'(12)–C'(13)	120(1)	N''(01)–C''(12)–C''(13)	124(1)
C(09)–N(10)–C(11)	117(1)	C'(04)–C'(13)–C'(05)	124(1)	C''(11)–C''(12)–C''(13)	119(1)
N(10)–C(11)–C(12)	116(1)	C'(04)–C'(13)–C'(12)	117(1)	C''(04)–C''(13)–C''(05)	121(1)
N(10)–C(11)–C(14)	121(1)	C'(05)–C'(13)–C'(12)	119(1)	C''(04)–C''(13)–C''(12)	117(1)
C(12)–C(11)–C(14)	122(1)	C'(06)–C'(14)–C'(07)	125(1)	C''(05)–C''(13)–C''(12)	123(1)
N(01)–C(12)–C(11)	121(1)	C'(06)–C'(14)–C'(11)	118(1)	C''(06)–C''(14)–C''(07)	123(1)
N(01)–C(12)–C(13)	123(1)	C'(07)–C'(14)–C'(11)	116(1)	C''(06)–C''(14)–C''(11)	120(1)
C(11)–C(12)–C(13)	116(1)	N(200)–C'(15)–C'(09)	111(1)	C''(07)–C''(14)–C''(11)	117(1)
C(04)–C(13)–C(05)	127(1)			N(200)–C''(15)–C''(09)	112(1)
C(04)–C(13)–C(12)	114(1)				
C(05)–C(13)–C(12)	119(1)			Cl(21)–C(20)–Cl(22)	111(1)
C(06)–C(14)–C(07)	122(1)			Cl(21)–C(20)–Cl(23)	110(1)
C(06)–C(14)–C(11)	119(1)			Cl(22)–C(20)–Cl(23)	111(1)
C(07)–C(14)–C(11)	119(1)			Cl(31)–C(30)–Cl(32)	112(1)
N(200)–C(15)–C(09)	113(1)			Cl(31)–C(30)–Cl(33)	110(1)
N(100)–C'(00)–C'(02)	113(1)			Cl(32)–C(30)–Cl(33)	112(1)

Table 6. Best Planes for the Phenanthroline Groups in **2 Br · 2CHCl₃**. The equation is given as Ax + By + Cz = D.

	A	B	C	D
Phen	– 0.9647	0.0136	– 0.2631	– 1.6977
Phen'	0.6350	0.0022	– 0.7725	– 1.5516
Phen''	– 0.3008	– 0.7236	– 0.6212	– 10.6412

The structure contains two CHCl₃ molecules. One is ordered and has the expected dimensions [7] of C–Cl_{aver} = 1.752(10) Å, uncorrected for thermal motions, and Cl–C–Cl = 110.6(3)° (Table 5). The second CHCl₃ molecule has very large apparent thermal motions with amplitudes ranging from 0.34 Å for 0(30) up to 0.74 Å for Cl(33). This results in shortened C–Cl distances averaging 1.69(2) Å.

A projection of the unit-cell upon the *ac* plane is shown without H-atoms on Fig. 2. All intermolecular contacts have normal distances.

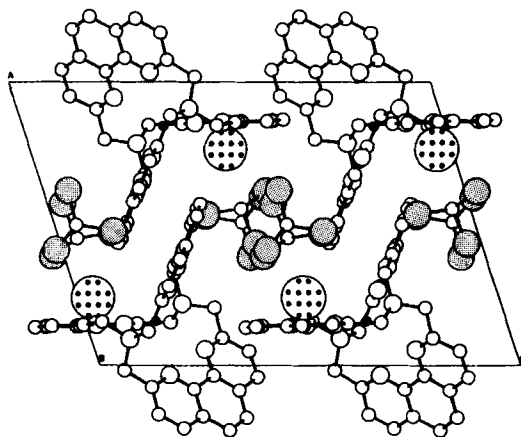


Fig. 2. Projection of the unit-cell upon the *ac*-plane

Structural Features of the Cryptate Cation 2. – The cryptate $[\text{Na}^+ \subset \mathbf{1}]$ is a very large organic cation having an average radius of about 5.7 Å (7.9 Å along the phenanthroline blades and 2.35 Å between them). The counterion Br^- is separated from the Na^+ cation by a distance of 6.9 Å. It is thus the largest cation among the spheroidal cryptates [3] [8]. As a consequence, it may further exalt the effects (cation protection, anion activation) which cryptate formation has been shown to have on a number of physical and chemical properties (ionic interactions, redox potentials, solvation, ionic reactivity) [8].

The propeller-shaped form of the complex cation (*Fig. 1*) agrees with the observation of non-equivalent CH_2 protons in the $^1\text{H-NMR}$ spectrum. The conformational process which makes these protons equivalent consists in a torsion around the bridgehead $\text{N} \cdots \text{N}$ axis resulting in the interconversion of the two forms of opposite (left-handed and right-handed) helicity. The rigidity of the phenanthroline groups accounts for the high coalescence temperature (320 K) and high energy barrier found for this process [1]. A similar twisting motion had already been observed in the earlier cryptands and cryptates with however a much lower energy barrier due to their lesser rigidity [9].

In the cryptate cation **2**, the Na^+ ion is located at the focal point of the dipole moments of the N sites. The rigidity of the Phen sites (and to a lesser extent of the bipy unit in analogous ligands [1]) imposes a constrained cavity to the free ligand **1** and directs the pyridine N sites into it. This should confer characteristic features (stability, selectivity, electrochemical and photochemical properties, *etc.*) to the complexes formed with both non-transition and transition metal ions.

We thank the CNRS and CEA-ORIS for financial support.

Experimental Part

The NaBr complex of 2,2',2'',9,9',9''-Bis[nitrilotri(methylene)]tris(1,10-phenanthroline) ($= [\text{phen} \cdot \text{phen} \cdot \text{phen}]$, **1**) [1] was crystallized from a CHCl_3 soln. giving pale yellow parallelepipedic platelets.

Crystal Data: $\text{C}_{42}\text{H}_{30}\text{N}_8 \cdot \text{NaBr} \cdot 2\text{CHCl}_3$, $M = 988.4$, monoclinic, space group $P2_1/c$, $a = 13.454(5)$, $b = 17.608(5)$, $c = 19.098(5)$ Å, $\beta = 107.67(3)^\circ$, $V = 4311$ Å³, $Z = 4$, $d_{\text{calc}} = 1.523$ gcm⁻³, $\lambda(\text{CuK}\alpha)$.

A crystal of dimensions $0.05 \times 0.20 \times 0.15$ mm was mounted unsealed on a four-circle diffractometer *Philips PW100*, and 3134 unique reflections with $I_{\text{obs}} > 2.5 I$ were measured and collected.

The intensities were then treated in the usual fashion and corrected for absorption by the empirical method of *Walker and Stuart* [10]. The Br^- ion was easily located by the *Patterson* method. Subsequently, all the other atoms were located unambiguously with successive difference synthesis maps, calculated initially with the bromide phases. Cyclic least-squares calculations [11], with up to six diagonal blocks, were used to refine the anisotropic temperature factors and the positional parameters of 22 located H-atoms with a constant temperature factor ($U_{\text{H}} = 0.05 \text{ \AA}^2$). The contribution from nine additional H-atoms was subsequently included by placing them at theoretical positions ($\text{C-H} = 1 \text{ \AA}$, $U_{\text{H}} = 0.05 \text{ \AA}^2$) and allowing them to ride the appropriate C-atoms until the end of the refinement. The final *R* factor reached a value of 9.2% with the 3334 non-zero unique reflections³).

In the course of the refinement it became clear, because of its large temperature factors and short bond lengths, that one CHCl_3 molecule was disordered. The possibility that it had partly sublimed was discounted since, among other factors, no decline in intensities could be detected over the ten-day recording period. To account for the disorder, refinement calculations were made alternatively with three isotropic CHCl_3 molecules of constant ideal geometry, each with an occupation factor of one third, slightly different orientations and variable C-positions, initially separated by 0.45 \AA , as suggested by the difference *Fourier*. However, since the ensuing *R* factor (9.0%) did not improve appreciably and the structure did not change materially, this complex disorder model was discarded.

REFERENCES

- [1] J. C. Rodriguez-Ubis, B. Alpha, D. Plancherel, J. M. Lehn, *Helv. Chim. Acta* **1984**, *67*, 2264.
- [2] B. Dietrich, J. M. Lehn, J. P. Sauvage, *Tetrahedron Lett.* **1969**, 2889; *Tetrahedron* **1973**, *29*, 1647.
- [3] J. M. Lehn, *Structure Bonding* **1973**, *16*, 1; *Acc. Chem. Res.* **1978**, *11*, 49.
- [4] B. Metz, D. Moras, R. Weiss, *J. Chem. Soc., Chem. Commun.* **1971**, 444.
- [5] D. L. Hughes, *J. Chem. Soc., Dalton Trans.* **1973**, 2347.
- [6] S. Nishigaki, H. Yoshioka, K. Nakatsu, *Acta Cryst. Allogr., Sect. B* **1978**, *34*, 875.
- [7] L. E. Sutton, 'Tables of Interatomic Distances and Configuration in Molecules and Ions', The Chemical Society, Burlington House, London W. 1, 1965, Supplement 1956–1959, Special Publication No. 18.
- [8] J. M. Lehn, *Pure Appl. Chem.* **1980**, *52*, 2303.
- [9] B. Dietrich, J. M. Lehn, J. P. Sauvage, J. Blanzat, *Tetrahedron* **1973**, *29*, 1629.
- [10] N. Walker, D. Stuart, *Acta Crystallogr., Sect. A* **1983**, *39*, 158.
- [11] G. M. Sheldrick, *SHELX 76 Program for Crystal Structure Determination*, Univ. of Cambridge, England, 1976.

³) The atomic parameters are available from the Director of the *Cambridge Crystallographic Data Center*, University Chemical Laboratory, Lensfield Road, Cambridge CB2 1EW. The list of observed and calculated structure factors is available from the authors at the Institut de Chimie des Substances Naturelles. Any request should be accompanied by the full literature citation.